

# Indoor and Outdoor Tests for a Chemi-capacitance Carbon Nanotube Sensor Installed on a Quadrotor Unmanned Aerial Vehicle for Dimethyl Methylphosphonate Detection and Mapping

Jong-Seon Kim,<sup>\*,‡</sup> Myeong Jae Lee,<sup>‡</sup> Hyunwoo Nam, Sangwon Do, Jae Hwan Lee, Myung Kyu Park, and Byeong Hwang Park



Cite This: *ACS Omega* 2021, 6, 16159–16164



Read Online

ACCESS |



Metrics & More

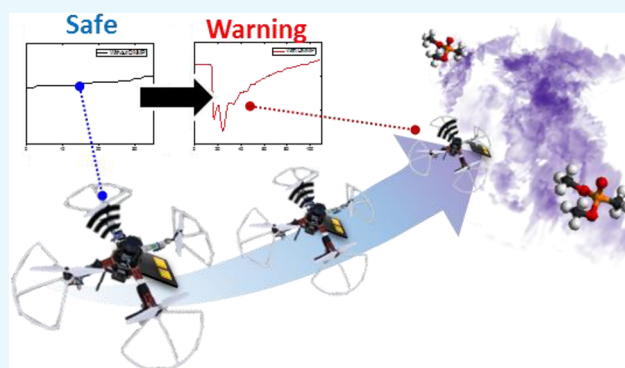


Article Recommendations



Supporting Information

**ABSTRACT:** Unmanned aerial vehicles (UAVs) have been used as a new chemical reconnaissance platform in chemical, biological, radiological, and nuclear detection and in industrial monitoring and environmental research, owing to their mobility, unconventional accessibility, and safety. Based on the UAV's payload and operational time considerations, the ultralight chip-sized chemical sensor is the most promising candidate for chemical reconnaissance among various chemical sensors. To optimize the UAV's chip-sensor performance, realistic outdoor tests of chemical sensors during UAV flights have to be conducted to verify their performances. In this study, indoor and outdoor experiments were conducted with a carbon nanotube (CNT)-based chip sensor installed on the UAV to detect dimethyl methylphosphonates (DMMPs), commonly used as chemical warfare agent simulants. Based on the indoor tests, DMMP concentrations and the position/direction of the CNT sensor were analyzed to optimize the sensing performances during UAV operations. Based on outdoor tests, we confirmed that the chemical sensor mounted on the UAV could detect DMMP gases by moving designated pathways in realistic conditions.



## 1. INTRODUCTION

Early detection and real-time monitoring of hazardous chemical materials are very important for avoiding disasters in military,<sup>1–3</sup> geological,<sup>4–6</sup> and industrial applications.<sup>7,8</sup> To maximize the detection capacity of the chemical sensor, it is essential to develop an efficient reconnaissance platform that can transport the sensor system within a nearby detectable range. Recently, considerable interest has been generated for the use of unmanned aerial vehicles (UAVs) as a state-of-art reconnaissance platform because of the speed, capacity to conduct flight missions without the engagement of humans, and high accessibility characteristics.<sup>9</sup>

Given the tremendous interest on UAVs, numerous technical advances have been accomplished regarding UAVs, including hardware (hydrodynamics design, low-weight batteries, position controlling sensor, and rotors) and software (flight controller, user graphical user interface, networking, and automatic driving).<sup>10–13</sup> Despite the rapid technological UAV improvements, the UAV payload remains the biggest concern in this area.<sup>14,15</sup> The operation time of commercialized UAVs (quadrotor type) is approximately 30–60 min and depends on the payload owing to battery capacity limitations. Various types of sensor systems have been suggested, including ion mobility spectrometry (IMS)<sup>16</sup> and hyperspectral Fourier transform

infrared spectroscopy (FTIR),<sup>17</sup> and chip-based sensors such as metal oxide sensors, electrochemical cells, and gravimetric sensors<sup>18,19</sup> are particularly interesting because they are ultralightweight, cheap, and replaceable. These properties make them highly desirable for stable and prolonged chemical reconnaissance missions in conjunction with the use of UAVs.

Javey's group developed a MOSFET-based chip sensor with microdrones for hydrogen detection,<sup>20</sup> while Marco's group conducted indoor ethanol source localization and mapping research with a metal-oxide-based chemiresistor sensor, which was placed on a commercial microdrone.<sup>9</sup> Brunelli's group suggested operational mode named butterfly for effective chemical detection with UAVs.<sup>21</sup> However, their research work confined to indoor or fumehood tests. Shigaki's group also reported the experimental evaluation of odor with pocket-sized quadcopter.<sup>22</sup> Additionally, Neumann's group reported an

Received: April 20, 2021

Accepted: June 1, 2021

Published: June 10, 2021



algorithm and practical wind tunnel and outdoor test for gas source localization (GSL).<sup>23,24</sup> Previous researches showed that small-sized UAV and lightweight sensing technologies will be promising candidates for a chemical reconnaissance platform. To improve the chemical reconnaissance UAV system, further researches should be conducted by considering variation and interference in indoor/outdoor.

Herein, we report indoor and outdoor test results with CNT-based chemical sensors with UAV systems to detect dimethyl methylphosphonate (DMMP) gas, commonly used as a simulant nerve gas agent.<sup>25</sup> The CNT-based chemi-capacitance sensor was provided by Sensortech Inc. in the Republic of Korea. It can detect DMMP by changing its capacitance through the CNT-based channel. CNT channels were coated with organic materials, which have high affinities to the organophosphorus functional group and help increase the sensitivity and selectivity performances of the chemi-capacitance sensor. As shown in Figure 1a, chemi-capacitance

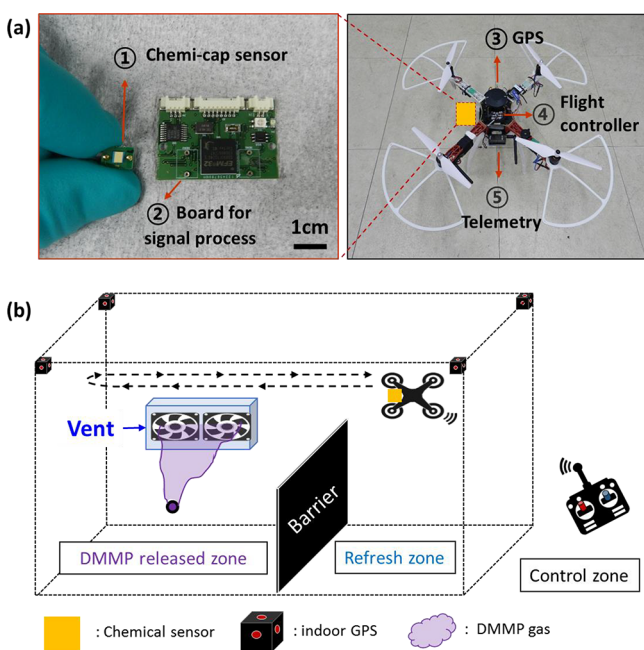


**Figure 1.** Imagery of a chemical sensor with an integrated circuit for signal processing on the customized unmanned aerial vehicle (UAV) and schematic drawing of the indoor dimethyl methylphosphonates (DMMP) release test facility. (a) Images show the chip-size chemical sensor and signal processing board (left), components, and sensor attachment position on the customized UAV (right). (b) Illustration of the setup conditions of the indoor DMMP exposure test facility used for the chemical sensor installed on the UAV.

sensor is small size (10 mm × 7 mm) and combined with a circuit board for signal process with UAVs. The CNT chemical sensor system was installed on our customized UAVs that consisted of a Pixhawk 2.1 flight controller (FC), a global positioning system (GPS) receiver, and a telemetric system for signal networking with the ground control system (GCS) that is described in Figure 1a. The UAV was executed on a laptop for recording flight information and collecting sensor data.

We combined the CNT sensor and UAV as a DMMP detection system and tested it indoors (Figure 1b) to optimize the sensor's position and orientation to maximize the detection performance against rotor flow effects. To map the DMMP detection from the sensor, we conducted indoor GPS-based

tests to analyze the sensor mapping performance. Based on the indoor test result, outdoor DMMP detection tests were also conducted in our approved test grounds.

## 2. EXPERIMENTS

Based on a previous particle image velocimetry (PIV) study (see Figure S1 in the Supporting Information), we confirmed that our UAV had a stable airflow region at the side of the main frame during rotor operations.<sup>26</sup> The main purpose of the indoor test was to identify the optimized sensor position and orientation at the side of the main frame. We recorded all the data and UAV trajectories from all the experiments to find the sensor's response at specific UAV locations. First, we conducted basic DMMP detection tests by moving the UAV forward and backward. Our UAV, which was equipped with the CNT sensor departed from the refresh zone, flew toward the DMMP zone, and then returned to the refresh zone, as shown in Figure 2a–d. The velocity of the UAV was also a

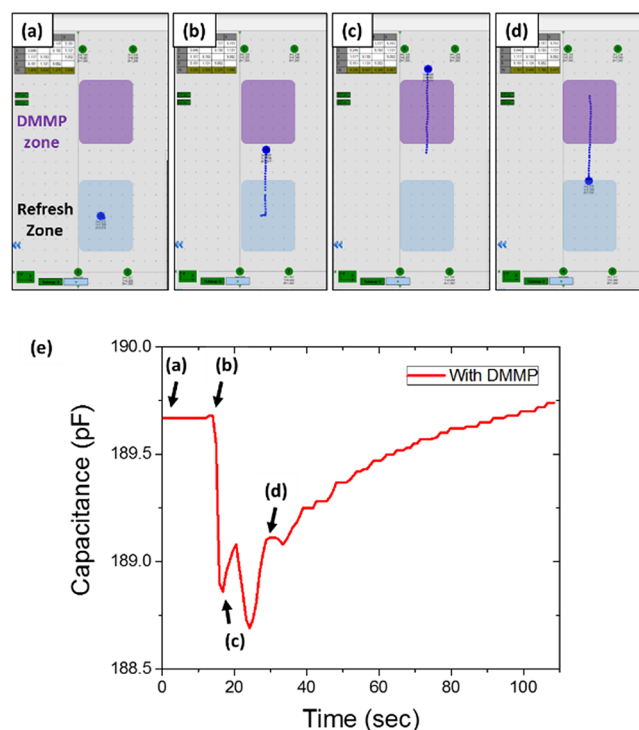


**Figure 2.** (a–d) Overall trajectory of the UAV recorded by indoor GPS system and (e) relevant DMMP detection graph of the CNT sensor.

controllable factor in the conducted experiments. However, in this case, the velocity of the UAV was fixed at a moderate speed (0.4 m/s) to monitor the sensor's signal and GPS position. When the UAV flew through the boundary of the DMMP zone, the CNT sensor immediately yielded the response depicted in Figure 2e. When the UAV arrived at the end of the DMMP zone, the CNT sensor recovered. This shows that DMMP gases are uniformly exhausted through the ventilation fan system. After the recovery of the CNT sensor at location (c), UAVs penetrated in the DMMP zone again. The second response of the CNT sensor was recovered when the UAV arrived at the refresh zone, as shown in Figure 2d. The CNT sensor recovered its own capacitance level as much as before the test. With repeated forward and backward tests, we

confirmed that the gas generation was uniform and the sensor could be fully recovered in the refresh zone (see Figure S2 in the Supporting Information).

### 3. RESULT AND DISCUSSION

#### 3.1. Indoor Tests. 3.1.1. Optimum Sensor Position.

Preliminary DMMP detection tests in Figure 2 were conducted with the use of the CNT sensor, which was installed at the front side of the UAV system.

To compare the response time of each position in Figure 3a, we conducted tests by rotating the position of the CNT sensor

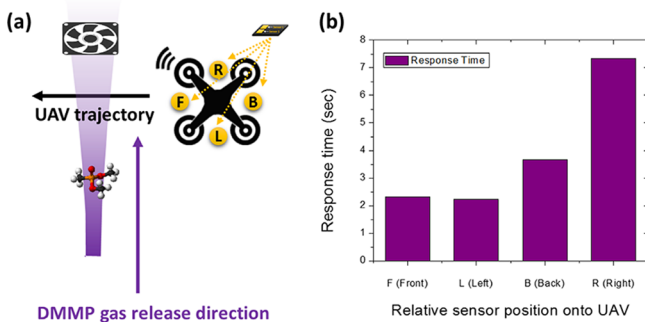


**Figure 3.** Schematic showing the positions of the chemical sensor with respect to the DMMP gas release direction and the corresponding response time graph. (a) Response times were measured at four different positions (front, back, left, and right) during the UAV's flight through the DMMP gas cloud. (b) The response time of the chemical sensor-equipped UAV in moving motion depended on different sensor positions.

against the DMMP gas. As a chemical reconnaissance platform, it is reasonable to assume that the UAV will operate to penetrate the DMMP gas cloud, as described in Figure 3a. Based on this hypothesis, four different sensor positions (front, left, right, and back) were selected as possible positions for the installation of the CNT sensor on the UAV. All the experiments were conducted with the same DMMP release conditions (rate of syringe pump for DMMP release and operation options (velocity, height, and trajectory of the UAV)). The UAV moved forward and backward through the UAV trajectory described in Figure 3a. All the response times were calculated from the baseline to the time period that yielded the highest DMMP peak. As shown in Figure 3b, the front and left sides showed relatively faster response times compared with the others. All the positions had increased DMMP detection capacities. However, there was a time delay with these structural disadvantages that led to the DMMP blocking effect that could decrease the DMMP concentration at each position. After this comparison, we tested the sensors, which were attached on the front side of the UAV to allow the execution of additional tests.

**3.1.2. Optimum Sensor Orientation.** Figure 4 illustrates different attachment orientations (horizontal, perpendicular, and upended) of the CNT sensor at the front of the UAV. It is worth noting that different orientations of the CNT sensor circuit against the DMMP gas flow may be used to provide more efficient molecular adsorption on the CNT bundles to generate high-capacitance changes for target DMMP gases. Among the three tested orientations, the perpendicularly attached sensors yielded faster response time characteristics compared with other sensor orientations. However, as

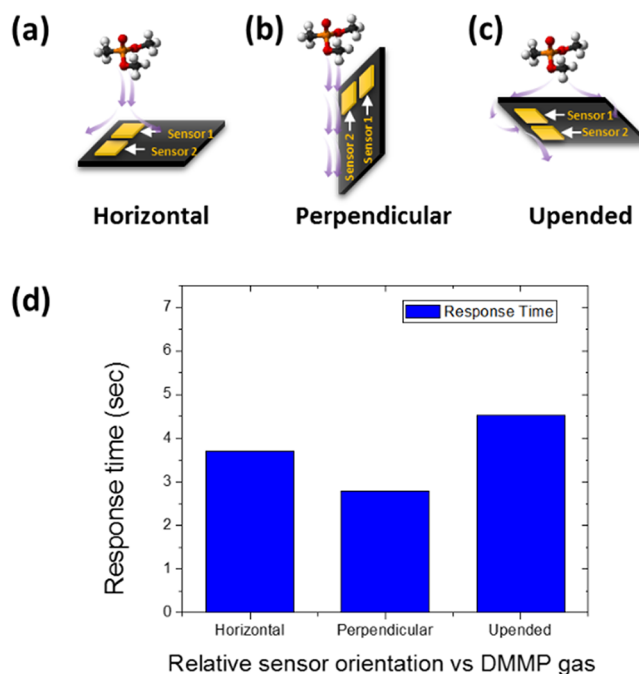


**Figure 4.** Schematic drawing about orientation change of the chemical sensor circuit against the DMMP flow (a–c). Rotation of rotor generates downstream gas flow near the sensor circuit as shown in schematic drawing. In the same DMMP releasing condition, the response time of the perpendicular orientation of the chemical sensor onto the UAV shows a faster response than other conditions (d).

indicated by previous experimental tests, the sensor's orientation is not as important as its location. Based on the aerodynamic analyses conducted in our own research studies (Supporting Information S1), the airflow was mainly streamed from the top to the bottom when the rotor was on. For this reason, the perpendicular sensor orientation enabled the maximization of the adsorbed DMMP molecules on the surface of the CNT bundle. The horizontal orientation also yielded a moderate response time for the DMMP gas, but the upended orientation of the CNT sensor yielded a slow response time in the same tests. From a detection viewpoint, the structural hindrance of the circuit board was not a major concern for the use of the UAV for the detection of hazardous chemicals. However, if we want to obtain mapping information for leaked chemicals or identify the leakage point from chemical reconnaissance UAV, the response time should be reduced as much as possible for real-time monitoring.

**3.1.3. Operational Height Comparison.** Most of the chemical gases are colorless. Therefore, the operation flight height should be given attention to maximize the sensor performance. Before the chemical reconnaissance, the user has to choose the UAV pathway to survey the expected contamination area. It is very challenging to specify an efficient pathway without any information on the gas leakage location. Therefore, an efficient UAV operational protocol can potentially enable an optimum gas detection pathway in a definite UAV flight time. To identify the operational effect at different UAV heights and target chemical clouds, the total capacitance change ( $\Delta$  capacitance) was measured as a function of the UAV height and with respect to the gas cloud. With the use of the same DMMP releasing conditions, we controlled the relative height of the UAV (defined as high (H), middle (M), or low (L)) to compare capacitance changes.



We assumed that the airflow from the rotor generated downstream when the UAV approaches the gas cloud and it could become a hindrance in the case in which the UAV would approach the gas cloud from a higher position. The maximum capacitance changes of the CNT sensor—that depend on the relative height between the UAV and the DMMP cloud—were measured and constituted typical indicators of the DMMP concentration changes near the CNT sensor. Because our demonstrations were conducted in an open fume hood, the maximum intensity would not represent the exact quantitative DMMP concentration. However, the CNT sensor has linearity and repeatability with DMMP (see Figure S3 in the Supporting Information). As shown in Figure 5, we measured the

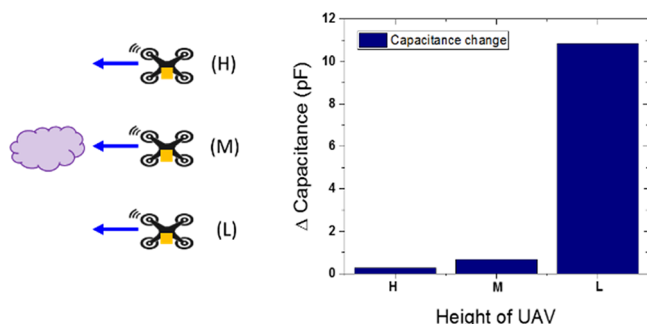


**Figure 5.** Measurements of the  $\Delta$  capacitance of the chemical sensor as a function of the relative height between the UAV and DMMP cloud (H, M, and L).

maximum capacitance change at different UAV positions to determine the effect of the relative height when the gas cloud needed to be detected during the UAV flying mode. Based on this experiment, we determined that an approach from the bottom of the cloud could result in a higher concentration sensor gas exposure compared with other approaches. It is very important to input an efficient UAV chemical reconnaissance pathway in realistic operations. Despite the fact that other approaches yielded worse detection performances regarding the DMMP gases, the signal-to-noise ratios were adequate to trigger the detection alarm. However, if we consider the outdoor conditions, such as wind, large survey areas would constitute critical issues regarding detection. Therefore, we concluded that a lower approaching chemical survey mode is a much efficient survey mode regarding the use of the UAV equipped with a chip-based sensor.

**3.1.4. Gas Cloud Boundary Detection.** Based on previous DMMP detection responses of the CNT sensor in the DMMP cloud, we think that the mapping of the DMMP cloud boundary is feasible with our UAV system. To test our hypothesis, we first conducted smoke emitting tests by changing the ventilation fan velocity (Regin Corporation, 45 s emitter). We observed subtle differences with the naked eye depending on the velocity, but it is impossible to measure the cloud difference by acquiring images. By controlling the velocity of the ventilation fan, we tried to generate different DMMP cloud sizes in the DMMP releasing zone.

Consecutive responses toward the DMMP gas with respect to the fan velocity (250–1500 revolutions per minute (rpm)) were measured to investigate the mapping ability of the CNT sensor on the UAV and the cloud boundary measurement ability. Figure 6 depicts consecutive response of the CNT sensor toward the DMMP gas at various fan velocities. From a

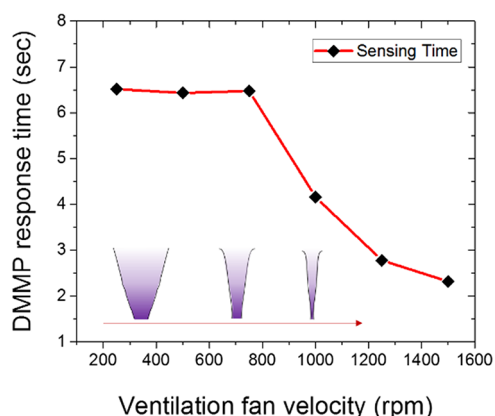


**Figure 6.** Measurement of DMMP response time as a function of the ventilation fan velocity from 250 to 1500 rpm.

fan velocity of 250–750 rpm, there were no noticeable changes in the DMMP response time because extra DMMP gases were evacuated with the use of fume hoods. As the fan velocity increased, we confirmed that the DMMP response times of the CNT sensor drastically decreased. This decreased the response time of the CNT sensor. This effect may be attributed to the gas cloud boundary. Boundary detection ability of the CNT sensor on the UAV implies that mapping of chemical cloud would be enabled with multiple operations of reconnaissance UAVs.

**3.2. Outdoor Test.** Distinctive sensing ability depends on the position, orientation, and approaching height of the UAV. All these parameters were investigated based on indoor tests in well-controlled and organized conditions. To clarify the practical capacity of the UAV as a chemical reconnaissance platform, we conducted outdoor DMMP detection tests in our approved ground. As shown in Figure 7a, we prepared a large testing area to ensure the safety of the experimenters. Additionally, we installed the indoor GPS poll and the receivers to acquire accurate GPS positions to generate the DMMP detection map, as shown in Figure 7b,c. The GCS system was lined up at the controlled zone (rectangle outlined with a blue dashed line in Figure 7a), and the UAVs and

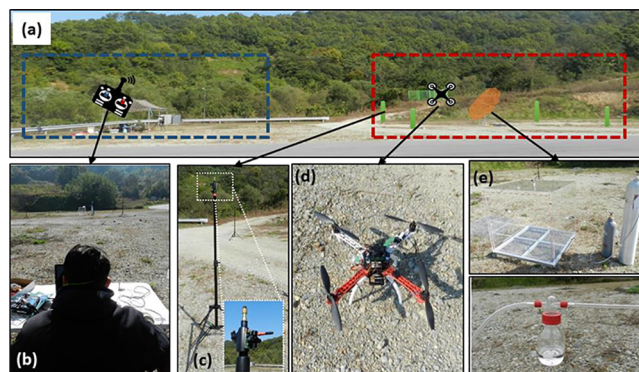


**Figure 7.** Experimental testing section of the outdoor test in proving grounds. (a) The rectangular box depicted in a blue dashed line is the controlled zone for the experimenter, and the rectangular box depicted in a red dashed line is the DMMP release zone used for UAV testing. (b) Experimenter's view (we obtained the consent of the depicted person) and (b, c) indoor GPS poll and GPS receiver used to measure accurate GPS signals from the UAV. (e) DMMP gas bubbling system and air gas cylinder used to release the DMMP gas.

DMMP gas generation system were installed in the release zone at the red dashed rectangular side in Figure 7a,d,e.

DMMP gas generation was achieved by heating the gas evaporation flask (Figure 7e) with a hotplate at approximately 200 °C. The evaporated DMMP gases propagated following the injection of air gas from the gas cylinder at a uniform gas flow (0.1 L/min). Because this was an outdoor test, the definition of the concentration of DMMP based on these experiments was difficult. The generated gases were first contained inside an acrylic box (described in Figure 7e) to achieve the stabilization of the released gas. After 1 min, we released DMMP at the designed Teflon tube, which was fixed 20 cm above the ground. When DMMP was released from Teflon tube, the UAV began its survey from the controlled to the released zones. Once it passed the contamination region, the CNT sensor measured the outdoor sensing ability of the UAV as a chemical reconnaissance platform.

Figure 8 shows the sensing response of the CNT sensor on the UAV in outdoor tests and its GPS mapping results as a

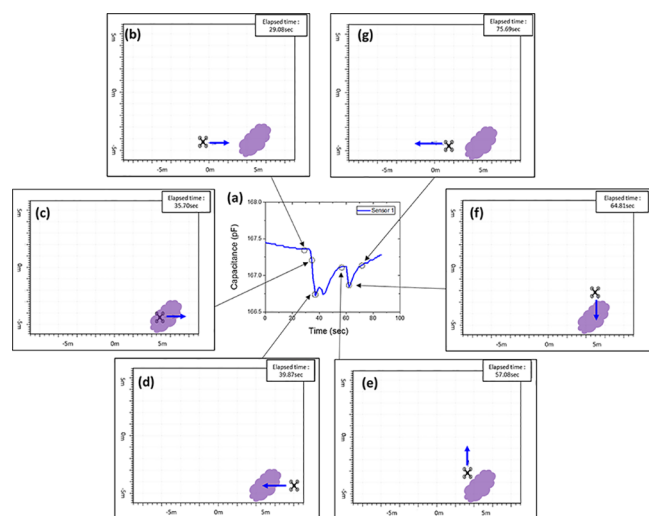


**Figure 8.** DMMP detection graph (a) and comparison of sensing CNT sensor response changes as a function of the UAV location in outdoor tests (b–g).

function of time. The UAV flight was the same as those used for indoor tests (and adopted forward to backward configurations) and passed through the DMMP gas release region. Additionally, we added a pathway to survey the contaminated region at the second reconnaissance when the UAV returned to its starting location. As shown in the DMMP detection graph in Figure 8a, the CNT sensor clearly exhibits two distinct chemical detection responses during the entire experimental periods of (a) 30 s devoted for forward reconnaissance and (b) 60 s devoted for backward reconnaissance. It shows a similar detection behavior with the indoor test result in Figure 2e. Comparison with the UAV's GPS signal indicated that the DMMP detection responses were highly consistent with the instances in which DMMP was released.

We developed customized software to monitor the two-dimensional trajectory of the UAV based on the GPS signal as a function of time (vertical X–Y plot of UAV trajectory). We quantified all the UAV positions that corresponded to the gas detection response and recovery responses shown in Figure 8a based on a recorded movie (see movie in the Supporting

information). As shown in Figure 8b–g, the UAV moved forward as indicated by the blue arrow in the map. When the UAV flew through the expected DMMP contamination region shown in Figure 8c, the sensor signal decreased abruptly. The UAV exhibited a minor recovery, as shown in Figure 8d, but the UAV flew into the DMMP cloud. As shown in Figure 8e, we input the additional mission trajectory for the surrounding survey in backward reconnaissance (second detection) so that the UAV would move to the upper side of the map. After the surrounding survey, the UAV re-entered the region that was contaminated by DMMP and then returned to the starting point, as depicted in Figure 8f,g. The distinct DMMP detection responses based on the outdoor tests demonstrated the feasibility of the UAV and chip-based sensor as the chemical reconnaissance platform in outdoor conditions.

## 4. CONCLUSIONS

We integrated and tested an UAV equipped with CNT-based chip-sized sensors in indoor and outdoor conditions. Based on the indoor tests, we optimized the position, orientations, and operating methods of the CNT sensor on the UAV for the monitoring of targeted gases (DMMP gas in this case considered as a Sarin agent simulant). The detection capacity of the CNT sensor on the UAV mainly depended on its attached position and the approaching height with respect to the DMMP cloud. During all the experiments, our UAV platform allowed accurate, fast monitoring of changes in DMMP concentration and facilitated the possibility of mapping in outdoor tests. Owing to the simplicity of the chip sensors, the sensor part of the UAV enabled the development of multiflexing systems and their applications on other target gases or reconnaissance missions where concentration changes constitute the critical indicator of disaster.

## ■ ASSOCIATED CONTENT

### Supporting Information

The Supporting Information is available free of charge at <https://pubs.acs.org/doi/10.1021/acsomega.1c02104>.

Video for two-dimensional mapping about the outdoor test with DMMP (MP4)

General information about PIV analysis about customized drone; repeatable DMMP detection result of CNT sensor; details of the sensor linearity (PDF)

## ■ AUTHOR INFORMATION

### Corresponding Author

Jong-Seon Kim – CBRN Directorate, Agency for Defense Development, Daejeon 34186, Korea; [orcid.org/0000-0003-3573-3442](https://orcid.org/0000-0003-3573-3442); Email: [kjs2636@add.re.kr](mailto:kjs2636@add.re.kr)

### Authors

Myeong Jae Lee – CBRN Directorate, Agency for Defense Development, Daejeon 34186, Korea

Hyunwoo Nam – CBRN Directorate, Agency for Defense Development, Daejeon 34186, Korea

Sangwon Do – CBRN Directorate, Agency for Defense Development, Daejeon 34186, Korea

Jae Hwan Lee – CBRN Directorate, Agency for Defense Development, Daejeon 34186, Korea

Myung Kyu Park – CBRN Directorate, Agency for Defense Development, Daejeon 34186, Korea

Byeong Hwang Park – CBRN Directorate, Agency for Defense Development, Daejeon 34186, Korea

Complete contact information is available at:

<https://pubs.acs.org/10.1021/acsoomega.1c02104>

### Author Contributions

<sup>‡</sup>J.-S.K. and M.J.L. contributed equally to this work.

### Notes

The authors declare no competing financial interest.

## ACKNOWLEDGMENTS

This work was supported by the Agency for Defense Development (ADD), Republic of Korea.

## REFERENCES

- (1) Kim, J.-S.; Nam, H.; Kim, H. J.; Lee, J. H.; Park, B. H. Real-time measurement of ammonia in artillery smoke using a passive FT-IR remote sensor. *ACS Omega* **2019**, *4*, 16768–16773.
- (2) Giannoukos, S.; Brkić, B.; Taylor, S.; Marshall, A.; Verbeck, G. F. Chemical sniffing instrumentation for security applications. *Chem. Rev.* **2016**, *116*, 8146–8172.
- (3) Jang, Y. J.; Kim, K.; Tsay, O. G.; Atwood, D. A.; Churchill, D. G. Destruction and detection of chemical warfare agents. *Chem. Rev.* **2015**, *115*, 5345.
- (4) Gao, M.; Xu, X.; Klinger, Y.; van Woerd, J.; Tapponnier, P. High-resolution mapping based on an unmanned aerial vehicle (UAV) to capture paleoseismic offsets along the Altyn-Tagh fault. *China. Sci. Rep.* **2017**, *7*, 8281.
- (5) Murfitt, S. L.; Allan, B. M.; Bellgrove, A.; Rattray, A.; Young, M. A.; Lerodiasconou, D. Applications of unmanned aerial vehicles in intertidal reef monitoring. *Sci. Rep.* **2017**, *7*, 10259.
- (6) Hodgson, J. C.; Baylis, S. M.; Mott, R.; Herrod, A.; Clarke, R. H. Precision wildlife monitoring using unmanned aerial vehicles. *Sci. Rep.* **2016**, *6*, 22574.
- (7) Feng, L.; Musto, C. J.; Kemling, J. W.; Lim, S. H.; Suslick, K. S. A colorimetric sensor array for identification of toxic gases below permissible exposure limits. *Chem. Commun.* **2010**, *46*, 2037–2039.
- (8) Seekaew, Y.; Pon-On, W.; Wongchoosuk, C. Ultrahigh Selective Room-Temperature Ammonia Gas Sensor Based on Tin–Titanium Dioxide/reduced Graphene/Carbon Nanotube Nanocomposites by the Solvothermal Method. *ACS Omega* **2019**, *4*, 16916–16924.
- (9) Burgués, J.; Hernández, V.; Lilienthal, A.; Marco, S. Smelling nano aerial vehicle for gas source localization and mapping. *Sensors* **2019**, *19*, 478.
- (10) Farlik, J.; Kratky, M.; Casar, J.; Stary, V. Multispectral detection of commercial unmanned aerial vehicle. *Sensors* **2019**, *19*, 1517.
- (11) Davies, L.; Bolam, R. C.; Vagapov, Y.; Anuchin, A. Review of unmanned aircraft system technologies to enable beyond visual line of sight (BVLOS) operations. *2018 X International conference on electrical power drive systems (ICEPDS)*; IEEE, 2018.
- (12) Citroni, R.; Leggieri, A.; Passi, D.; Paolo, F. D.; Carlo, A. D. Nano energy harvesting with plasmonic nano-antennas: a review of MID-IR rectenna and application. *Advanced Electromagnetics* **2017**, *1*.
- (13) Chen, H. X.; Nan, Y.; Yang, Y. Multi-UAV reconnaissance task assignment for heterogeneous targets based on modified symbiotic organisms search algorithm. *Sensors* **2019**, *19*, 734.
- (14) Mohiuddin, A.; Taha, T.; Zweiri, Y.; Gan, D. UAV payload transportation via RTDP based optimized velocity profiles. *Energies* **2019**, *12*, 3049.
- (15) Toksoz, T.; Redding, J.; Michini, M.; Michini, B.; How, J. P. Automated battery swap and recharge to enable persistent UAV missions; Infotech@Aerospace 2011, St.Louis, **2011**.
- (16) Cascio, J.; Hale, M.; Owens, A.; Swann, S.; Weliver, A.; Jimenez, J. Creating a decision support tool for the stryker NBC RV. *Proceedings of the annual general Donald R. Keith memorial conference; ieworldconference*, 2019. 124–129
- (17) Adão, T.; Hruska, J.; Pádua, L.; Bessa, J.; Peres, E.; Morais, R.; Sousa, J. J. Hyperspectral imaging: a review on UAV-based sensors, data processing and applications for agriculture and forestry. *Remote Sens.* **2017**, *9*, 1110.
- (18) Sørensen, L. Y.; Jacobsen, L. T.; Hansen, J. P. Low cost and flexible UAV deployment of sensors. *Sensors* **2017**, *17*, 154.
- (19) Burgués, J.; Marco, S. Environmental chemical sensing using small drones : A review. *Sci. Total Environ.* **2020**, *748*, 141172.
- (20) Fahad, H. M.; Shiraki, H.; Amani, M.; Zhang, C.; Hebbar, V. S.; Gao, W.; Ota, H.; Hettick, M.; Kiriya, D.; Chen, Y.-Z.; Chueh, Y.-L.; Javey, A. Room temperature multiplexed gas sensing using chemical-sensitive 3.5-nm-thin silicon transistors. *Sci. Adv.* **2017**, *3*, No. e1602557.
- (21) Rossi, M.; Brunelli, D. Gas sensing on unmanned vehicles: challenges and opportunities. *2017 New Generation of CAS (NGCAS)*; IEEE, 2017.
- (22) Shigaki, S.; Fikri, M.; Kurabayashi, D. Design and Experimental Evaluation of an Odor Sensing Method for a Pocket-Sized Quadcopter. *Sensors* **2018**, *18*, 3720.
- (23) Neumann, P. P.; Bennetts, V. H.; Lilienthal, A. J.; Bartholmai, M.; Schiller, J. H. Gas source localization with a micro-drone using bio-inspired and particle filter-based algorithms. *Adv. Rob.* **2013**, *27*, 725–738.
- (24) Neumann, P. P.; Asadi, S.; Lilienthal, A. J.; Bartholmai, M.; Schiller, J. H. *Micro-Drone for wind vector estimation and gas distribution mapping*; Journal of IEEE Robotics and Automation magazine, 2011. 6 (1).
- (25) Kim, W.; Lee, J. S. Freestanding and Flexible  $\beta$ -MnO<sub>2</sub>@Carbon Sheet for Application as a Highly Sensitive Dimethyl Methylphosphonate Sensor. *ACS Omega* **2021**, *6*, 4988–4994.
- (26) Do, S.; Lee, M.; Kim, J.-S. The Effect of a Flow Field on Chemical Detection Performance of Quadrotor Drone. *Sensors* **2020**, *20*, 3262.